

MR Findings of the Spinal Paraganglioma : Report of Three Cases

Extraadrenal paragangliomas involving the spine is less common and usually takes the form of intradural compression of the cauda equina. The authors report three cases of spinal paragangliomas resulting in extradural spinal cord compression and their MR findings. The MR imaging revealed a well-demarcated extradural mass with low to intermediate signal intensity on T1-weighted images and intermediate to high signal intensity on T2-weighted images compared to paravertebral muscles. After Gd-DTPA administration, heterogeneous and intense enhancement was found. Multiple punctate and serpiginous structures of signal void due to high-velocity flow were noted around and within the tumors on all sequences. In one case, the signal void structures were well corresponded with feeding arteries on angiography. These may be the characteristic findings of the extraadrenal paraganglioma involving the spine.

Key Words : Paraganglioma, Extraadrenal; Magnetic Resonance Imaging; Spine, Paraganglioma

Joo Yong Shin, Sung Moon Lee,
Mee Young Hwang*, Cheol Ho Sohn,
Soo Jhi Suh

Department of Diagnostic Radiology, Keimyung
University School of Medicine; Department of
Radiology*, Kaya Christian Hospital, Taegu, Korea

Received : 14 June 2000

Accepted : 21 October 2000

Address for correspondence

Sung Moon Lee, M.D.

Department of Diagnostic Radiology, Dongsan
Medical Center, Keimyung University School of
Medicine, 194 Dongsan-dong, Joong-gu, Taegu
700-310, Korea

Tel: +82-53-250-7767, Fax: +82-53-250-7766

E-mail: smlee@dsmc.or.kr

INTRODUCTION

Paragangliomas are tumors arising in the paraganglia. Extraadrenal paragangliomas are usually located in the head and neck region, with 90% arising in the carotid body or glomus jugulare (1). Involvement of the spine is less common and usually takes the form of intradural compression of cauda equina (2, 3). Epidural compression of the spinal cord by paraganglioma involving the spine occurs rarely, and only several cases have been previously reported (4-6). In addition, MR findings of spinal paraganglioma were not clearly described. We report three additional cases of spinal paragangliomas resulting in extradural cord compression and their MR findings with review of the literature.

CASE REPORT

Case 1

A 43-yr-old man was admitted, complaining of paresthesia of the lower extremities and urinary incontinence. Before admission, he had experienced intermittent upper back pain without radiating nature for one year.

Plain radiography revealed compression fracture of T6

vertebra with left paraspinal mass. CT scan showed compression fracture and osteolytic change involving both the pedicles, left transverse process, spinous process of T6 vertebra, and left sixth rib. The anterior epidural mass was compressing spinal cord and large inhomogeneous paraspinal soft tissue mass was surrounding the aorta. MR imaging was performed with a 1.5T magnet (Magnetom Vision, Siemens, Germany). MR images revealed expansile appearance of T6 vertebra with compression of the spinal cord and large paraspinal mass with inhomogeneous low to intermediate signal intensity on T1-weighted images and intermediate to high signal intensity on T2-weighted images compared to paravertebral muscle. There were multiple punctate and serpiginous structures of signal void around and within the mass on all sequences. After injection of Gd-DTPA, intense enhancement of the mass was noted (Fig. 1A, B). Angiography revealed multiple large feeding arteries and marked tumor blushes, originating from the left sixth, seventh, eighth, and right sixth intercostal arteries, and prominent draining veins (Fig. 1C). Preoperative embolization was performed with gel-foam particles. Microscopic examination revealed a well-differentiated neoplasm containing clusters of granulated epithelioid cells surrounded by thin fibrovascular stroma ("Zell-ballen"). Round to oval nuclei with finely granulated chromatin and prominent

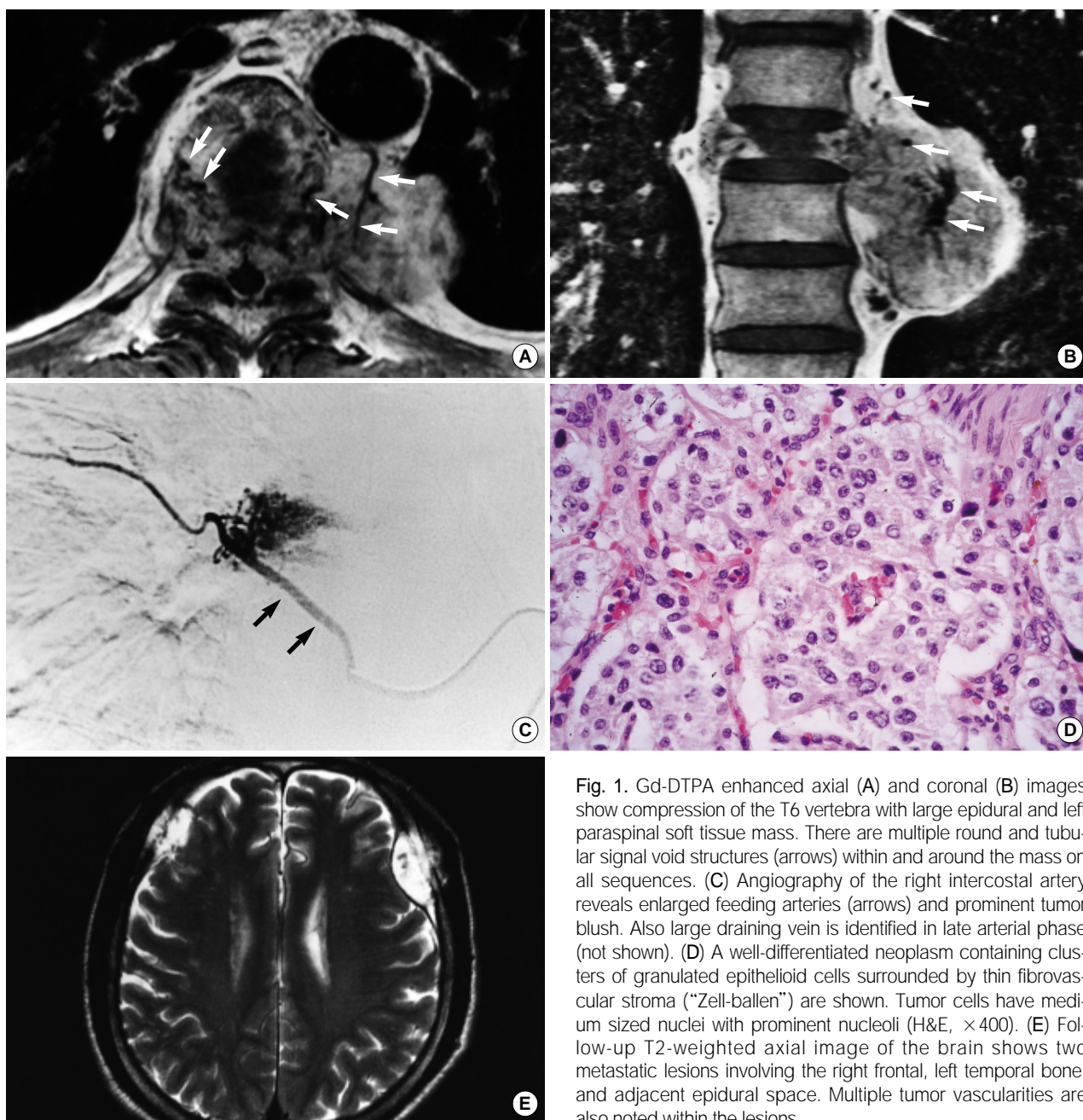


Fig. 1. Gd-DTPA enhanced axial (A) and coronal (B) images show compression of the T6 vertebra with large epidural and left paraspinal soft tissue mass. There are multiple round and tubular signal void structures (arrows) within and around the mass on all sequences. (C) Angiography of the right intercostal artery reveals enlarged feeding arteries (arrows) and prominent tumor blush. Also large draining vein is identified in late arterial phase (not shown). (D) A well-differentiated neoplasm containing clusters of granulated epithelioid cells surrounded by thin fibrovascular stroma ("Zell-ballen") are shown. Tumor cells have medium sized nuclei with prominent nucleoli (H&E, $\times 400$). (E) Follow-up T2-weighted axial image of the brain shows two metastatic lesions involving the right frontal, left temporal bone, and adjacent epidural space. Multiple tumor vascularities are also noted within the lesions.

nucleoli occupied the center of the cells (Fig. 1D). The structural features of the neoplasm were indicative of paraganglioma.

Six months later, he complained bifrontal headache of dull nature. MR images showed two metastatic lesions involving the right frontal, left temporal bones and the adjacent epidural space (Fig. 1E). These were also proved as paraganglioma and were finally diagnosed as malignant. Chemotherapy and radiotherapy were performed, but the outcome was not satisfactory.

Case 2

A 67-yr-old woman was presented with a history of band-like lower abdominal pain for one year and back pain for several years. Physical examination revealed tenderness on lower dorsal spinal area. The conventional radiograph of the thoracic spine demonstrated an osteolytic change involving the right pedicle, transverse and spinous process of T11. CT scan showed large homogeneous soft tissue mass involving the right pedicle, both laminae, spinous process, and right posterior portion of the body of T11 vertebra,

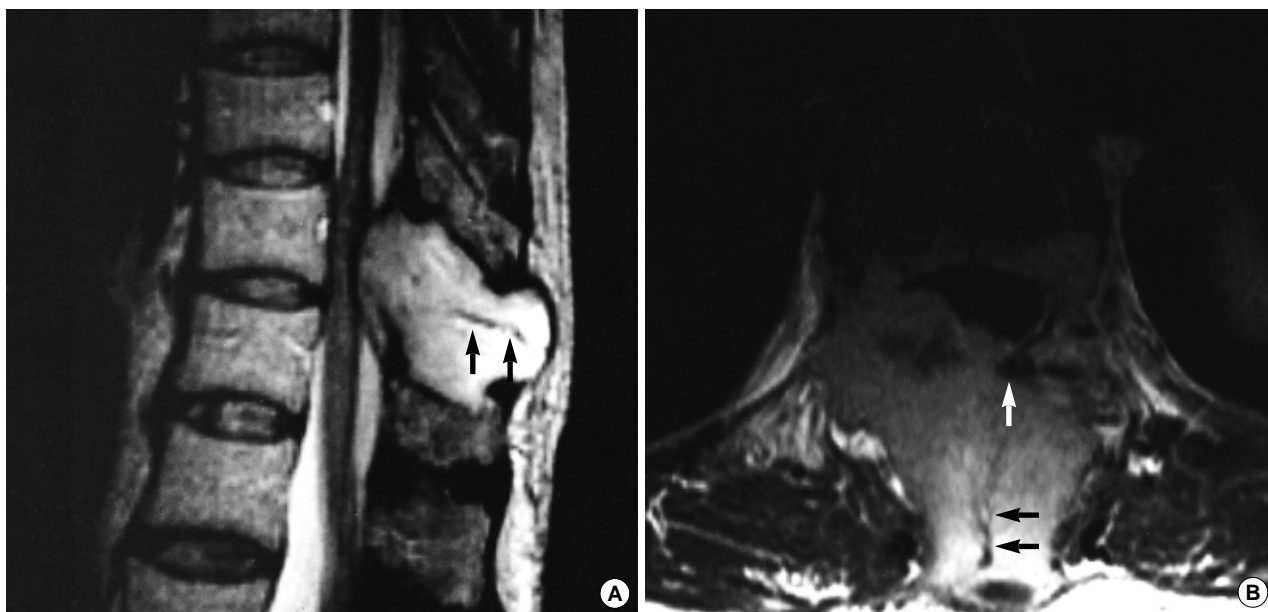


Fig. 2. T2-weighted sagittal (A) and Gd-DTPA enhanced axial (B) images show large lobulated mass involving posterior arch of T11 vertebra and posterior epidural mass. The mass is relatively well defined and intense enhancement. There are tree-like tubular and round signal void structures within the lesion (arrows).

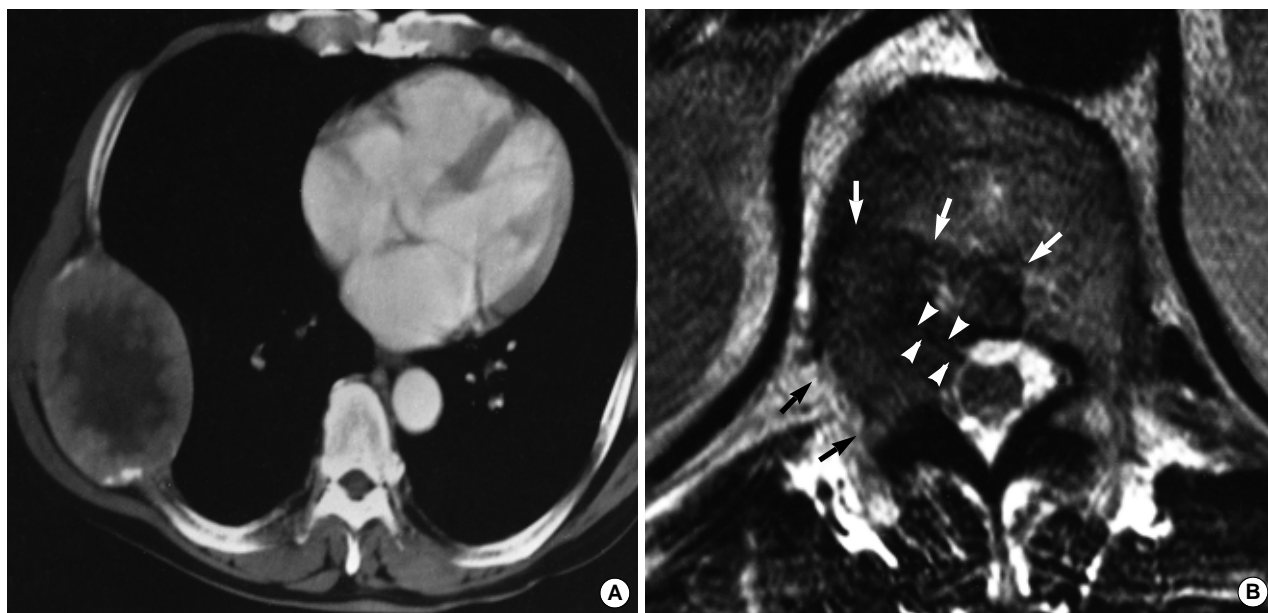


Fig. 3. (A) Enhanced chest CT scan reveals huge extrapleural mass with osteolytic change of right seventh rib. The mass has central irregular area of low-density that represents necrosis. High-density foci at peripheral margin of the mass are not enhancing vessels but small bony fragment. Enlarged tumor vessels are not seen on CT scan. (B) Two years later, axial T2-weighted image through T12 vertebra shows intermediate signal intensity mass involving the right posterior vertebral body and the pedicle with epidural mass (arrows). There are tubular signal void structures within the mass that may represent feeding arteries from the spinal artery (arrowheads).

which compresses the spinal cord. On MR images (1.0T, Magnetom Impact, Siemens, Germany), the mass revealed low signal intensity on T1-weighted images and inhomogeneous hyperintensity on T2-weighted images, with tubular signal voids around and within the mass (Fig. 2A).

Enhancement study with gadolinium-DTPA displayed intense patchy enhancement (Fig. 2B).

Thoracic laminectomy was performed for a posterior decompression of the spinal cord. $4 \times 4 \times 5$ cm sized epidural mass was highly vascular, and complete removal could

not be done because of massive tumor bleeding and wide involvement of the bony structures. The lesion was proved as paraganglioma.

Case 3

A 62-yr-old man was admitted due to palpable right chest wall mass. On physical examination, 10×8 cm sized, nontender, firmly fixed mass was noted. A plain chest radiograph demonstrated huge extrapleural mass with osteolytic change of right seventh rib. CT scan showed well defined, large, necrotic soft tissue mass arising from right seventh rib with osteolytic change (Fig. 3A). Bone scan with Technetium-99m disclosed a focal increased activity at the right seventh rib without other lesions. The histologic features were characteristic of paraganglioma.

Two years later, he had radiating pain to right hip and paresthesia of right lower extremity. MR imaging showed a destructive lesion of T12 body with soft tissue mass that resulted in cord compression. The mass showed homogeneous intermediate signal intensity on T1 and T2-weighted images. Tubular and dot-like signal void structures were noted in the periphery and within the mass (Fig. 3B). Focal heterogeneous enhancement was demonstrated after gadolinium administration. Multiple metastatic lesions were found also in T9, T11, and L2 vertebral bodies. CT-guided biopsy was performed at T12 and histologically diagnosed as paraganglioma.

DISCUSSION

Parangliomas are extra-adrenal rests of neural crest-derived cells that are closely associated with the autonomic nervous system and are found in widely dispersed locations in the head, neck, thorax and abdomen. These structures have been reported as chemoreceptors in some individuals and, possibly, as interneurons of the autonomic system in others (7). However, the distribution and role of cells derived from the neural crest outside the carotid and aortic bodies are poorly understood (8).

Parangliomas are tumors of the extra-adrenal paraganglion system and, in accord with the multicentricity of paraganglia, have been reported in many diverse locations, such as prostate (9), larynx (10), gall bladder (11), intrathoracic region (12), and spine (4-6). The proposed mechanism for the origin of such tumors involves considerably more extensive distribution of paraganglia in fetus or neonate (13). Presumably, spinal paragangliomas originate from the sympathetic neurons in the thoracic and lumbar lateral horns of the spinal cord, sending their axons to the sympathetic trunk through the communicating branches. It may also be possible that heterotopic neurons lie along these branches proximal to the sympathetic trunk (14).

Parangliomas are usually regarded as benign, but malignancy is found in 6.5% of all extraadrenal paragangliomas and local recurrence has been described in 12% (4, 7). Total excision and follow-up study are recommended because even metastatic specimens can initially appear as benign.

Parangliomas are characterized by the presence of two cell types, classically arranged into lobules or "Zell-ballen". The predominant cell type is the chief cell, which is round to oval in shape with abundant eosinophilic granular cytoplasm. The second cell type is the sustentacular or supporting cell. The loss of normal paraganglionic architecture in paragangliomas has been associated with more aggressive or malignant behavior. The paucity or absence of sustentacular cells in paraganglionic neoplasms has also been demonstrated to be an indicator of aggressive or malignant nature (1, 15).

The hypervascular nature of paragangliomas is a distinctive feature that has been noted on both angiography and MR imaging. This hypervascularity results in punctate areas of flow void interspersed in a matrix of increased signal intensity caused by slow flow and tumor cell; this produces a "salt-and-pepper" appearance on T2-weighted images. However, small tumors tend not to show the flow-void phenomenon (16). In our cases, all three cases showed tubular and dot-like signal void structures around and within the tumors that represent high velocity flow. In case 1, angiographic findings were well correlated with signal void structures on MR images. In other radiologic studies, however, these vascular structures are not identified, even on enhanced CT. Parizel et al. (17) stated that the enhanced MR image was particularly useful in accurately delineating the extent of the tumor. Heterogeneity seen on T2-weighted images was thought to reflect subacute and chronic hemorrhage.

The differential diagnosis of spinal paraganglioma includes metastases, multiple myeloma, and other highly vascular tumors. Differentiation of paragangliomas from these tumors is frequently not possible on MRI because of considerable overlap in their imaging findings. On our experience, other tumors involving the vertebral body, such as metastasis and multiple myeloma, have a less vascular appearance in their internal matrix. Angiolipoma usually shows focal fat component within the tumor. Hemangioma also presents with variable signal intensity and radiologic findings depending on its aggressiveness, but it usually reveals cortical expansion and prominent trabeculation with honeycomb pattern (17, 18).

In summary, paragangliomas of the spine revealed relatively well defined mass with low to intermediate signal intensity on T1-weighted images and intermediate to high signal intensity on T2-weighted images, compared to paravertebral muscles. Contrast-enhanced MR images showed intense heterogeneous enhancement. Multiple punctate and serpiginous areas of signal void due to high-velocity flow

are noted around and within the tumors in all three cases on all sequences. These may be the characteristic findings of spinal paraganglioma. In the spinal tumors, the possibility of paraganglioma should be included in differential diagnosis if there are prominent and abundant vascular structures within the matrix.

REFERENCES

1. Kliewer KE, Wen DR, Cancilla PA. *Paragangliomas: assessment of prognosis by histologic, immunohistochemical, and ultrastructural techniques. Hum Pathol* 1989; 20: 29-39.
2. Mylonas C. *Case report: paraganglioma of the cauda equina. Clin Radiol* 1992; 46: 139-41.
3. Reyes MG, Torres H. *Intrathecal paraganglioma of the cauda equina. Neurosurgery* 1984; 15: 578-82.
4. Fitzgerald LF, Cech DA, Goodman JC. *Paraganglioma of the thoracic spinal cord. Clin Neurol Neurosurg* 1996; 98: 183-5.
5. Solymosi L, Ferbert A. *A case of spinal paraganglioma. Neuroradiology* 1985; 27: 217-9.
6. Cybulski GR, Nijensohn E, Brody BA, Meyer PR Jr, Cohen B. *Spinal cord compression from a thoracic paraganglioma: case report. Neurosurgery* 1991; 28: 306-9.
7. Dial P, Marks C, Bolton J. *Current management of paragangliomas. Surg Gynecol Obstet* 1982; 155: 187-92.
8. Talbot AR. *Paraganglioma of the maxillary sinus. J Laryngol Otol* 1990; 104: 248-51.
9. Mehta M, Nadel NS, Lonni Y, Ali I. *Malignant paraganglioma of the prostate and retroperitoneum. J Urol* 1979; 121: 376-8.
10. Crowther JA, Colman BH. *Chemodectoma of the larynx. J Laryngol Otol* 1987; 101: 1095-8.
11. Miller TA, Weber TR, Appelman HD. *Paraganglioma of the gallbladder. Arch Surg* 1972; 105: 637-9.
12. Singh G, Lee RE, Brooks HD. *Primary pulmonary paraganglioma: report of a case and review of the literature. Cancer* 1977; 40: 2286-9.
13. Ho KC, Meyer C, Garancis J, Hanna J. *Chemodectoma involving the cavernous sinus and semilunar ganglion. Hum Pathol* 1982; 13: 942-3.
14. Sundgren P, Annertz M, Englund E, Stromblad LG, Holtås S. *Paragangliomas of the spinal canal. Neuroradiology* 1999; 41: 788-94.
15. Kliewer KE, Cochran AJ. *A review of the histology, ultrastructure, immunohistology and molecular biology of extra-adrenal paragangliomas. Arch Pathol Lab Med* 1989; 113: 1209-18.
16. Van Gils AP, van den Berg R, Falke TH, Bloem JL, Prins HJ, Dillon EH, van der Mey AG, Pauwels EK. *MR diagnosis of paraganglioma of the head and neck: value of contrast enhancement. Am J Roentgenol* 1994; 162: 147-53.
17. Parizel PM, Baleriaux D, Rodesch G, Segebarth C, Lalmand B, Christophe C, Lemort M, Haesendonck P, Niendorf HP, Flament-Durand J. *Gd-DTPA-enhanced MR imaging of spinal tumors. Am J Roentgenol* 1989; 152: 1087-96.
18. Laredo JD, Assouline E, Gelbert F, Wybier M, Merland JJ, Tubiana JM. *Vertebral hemangiomas: fat content as a sign of aggressiveness. Radiology* 1990; 177: 467-72.